

UCSF

UC San Francisco Previously Published Works

Title

p75 Neurotrophin Receptor Regulates Energy Balance in Obesity

Permalink

<https://escholarship.org/uc/item/87b491dw>

Journal

Cell Reports, 14(2)

ISSN

2639-1856

Authors

Baeza-Raja, Bernat

Sachs, Benjamin D

Li, Pingping

et al.

Publication Date

2016

DOI

10.1016/j.celrep.2015.12.028

Copyright Information

This work is made available under the terms of a Creative Commons Attribution-NonCommercial-NoDerivatives License, available at

<https://creativecommons.org/licenses/by-nc-nd/4.0/>

Peer reviewed



Published in final edited form as:

Cell Rep. 2016 January 12; 14(2): 255–268. doi:10.1016/j.celrep.2015.12.028.

p75 neurotrophin receptor regulates energy balance in obesity

Bernat Baeza-Raja¹, Benjamin D. Sachs², Pingping Li³, Frank Christian⁴, Eirini Vagena¹, Dimitrios Davalos¹, Natacha Le Moan¹, Jae Kyu Ryu¹, Shoana L. Sikorski², Justin P. Chan¹, Miriam Scadeng⁵, Susan S. Taylor^{2,6}, Miles D. Houslay⁷, George S. Baillie⁴, Alan R. Saltiel³, Jerrold M. Olefsky³, and Katerina Akassoglou^{1,8,*}

¹Gladstone Institute of Neurological Disease, University of California, San Francisco, CA 94158, USA

²Department of Pharmacology, University of California, San Diego, La Jolla, CA 92093, USA

³Department of Medicine, University of California, San Diego, La Jolla, CA 92093, USA

⁴Institute of Cardiovascular and Medical Sciences, University of Glasgow, Glasgow G12 8QQ, UK

⁵Department of Radiology, University of California, San Diego, La Jolla, CA 92093, USA

⁶Department of Chemistry and Biochemistry, University of California, San Diego, La Jolla, CA 92093, USA

⁷Institute of Pharmaceutical Science, King's College London, London SE1 9NH, UK

⁸Department of Neurology, University of California, San Francisco, CA 94158, USA

Summary

Obesity and metabolic syndrome reflect the dysregulation of molecular pathways that control energy homeostasis. Here we show that upon high-fat diet (HFD), the p75 neurotrophin receptor (p75^{NTR}) controls energy expenditure in obese mice. Despite no changes in food intake, p75^{NTR}-null mice were protected from HFD-induced obesity and remained lean due to increased energy expenditure, without developing insulin resistance or liver steatosis. p75^{NTR} directly interacts with the catalytic subunit of protein kinase A (PKA) and regulates cAMP signaling in adipocytes, leading to decreased lipolysis and thermogenesis. Adipocyte-specific depletion of p75^{NTR} or transplantation of p75^{NTR}-null white adipose tissue (WAT) into wild-type mice fed a HFD

*Correspondence: kakassoglou@gladstone.ucsf.edu (K.A.), Tel 415-734-2512, Fax 415-355-0824.

Supplemental Information: Supplemental Information includes Extended Experimental Procedures and fourteen Supplemental Figures.

Author Contributions: B.B-R. performed lipolysis, biochemical and gene expression analysis, fat transplantation experiments, and all in vivo studies with p75 conditional mice. B.D.S. and D.D. performed HFD weight and liver steatosis experiments. P.L. performed glucose and insulin tolerance tests and hyperinsulinemic-euglycemic clamps. E.V. and N.L.M. performed in vitro lipolysis and cAMP experiments. S.L.S. maintained mouse colonies and performed genotyping experiments. J.K.R. performed histological analysis. M.S. performed MRI analysis. F.C. designed, performed and analyzed ELISA binding assays and peptide arrays. A.R.S., J.M.O., S.S.T., and M.D.H. contributed to the experimental design, data analysis, and interpretation. B.B-R. and K.A. designed the study, analyzed data, coordinated the experimental work, and wrote the manuscript with contribution from all authors.

Publisher's Disclaimer: This is a PDF file of an unedited manuscript that has been accepted for publication. As a service to our customers we are providing this early version of the manuscript. The manuscript will undergo copyediting, typesetting, and review of the resulting proof before it is published in its final form. Please note that during the production process errors may be discovered which could affect the content, and all legal disclaimers that apply to the journal pertain.

protected against weight gain and insulin resistance. Our results reveal that signaling from p75^{NTR} to cAMP/PKA regulates energy balance and suggest that non-neuronal functions of neurotrophin receptor signaling could be a new target for treating obesity and the metabolic syndrome.

Introduction

Obesity, and the ensuing metabolic syndrome characterized by type 2 diabetes, hepatic steatosis, and atherosclerosis, is a worldwide epidemic that increases morbidity and mortality. Obesity develops when energy intake chronically exceeds energy expenditure (Spiegelman and Flier, 2001). While many factors control weight gain, glucose, and lipid metabolism (O'Rahilly and Farooqi, 2006), the molecular mechanisms that dysregulate energy balance remain poorly understood. By understanding these mechanisms, we can develop novel treatments for obesity and its comorbidities.

Studies on energy intake have identified several pathways that control appetite and hypothalamic functions, including leptin, neuropeptide Y, and melanocortin receptors (Spiegelman and Flier, 2001). Intriguingly, neurotrophin activation of cognate tyrosine kinase (Trk) receptors correlates with hypothalamic suppression of appetite control. Indeed, brain-derived neurotrophic factor (BDNF) signals through TrkB in the hypothalamus to suppress appetite and reduce body weight (Lyons et al., 1999; Xu et al., 2003b). On a normal diet, *BDNF*^{+/-} mice (Lyons et al., 1999) or mice conditionally-depleted of *BDNF* in neurons (Xu et al., 2003b) overeat and become obese. These results suggest that neurotrophin receptor signaling affects how the central nervous system (CNS) controls energy intake and body weight.

Neurotrophins and their receptors are also expressed in several peripheral metabolic tissues, suggesting that non-CNS molecular networks might regulate energy expenditure. Here, we report that loss of p75 neurotrophin receptor (p75^{NTR}) protects mice from obesity and the metabolic syndrome. p75^{NTR} regulates energy expenditure and thermogenesis and its adipocyte-specific depletion reduces obesity. These findings suggest that manipulating non-neuronal functions of p75^{NTR} signaling could provide a new therapeutic approach for obesity and the metabolic syndrome.

Results

p75^{NTR} Knockout Mice Are Resistant to HFD-Induced Obesity, Insulin Resistance, and Hepatic Steatosis

p75^{NTR} is widely expressed in metabolic tissues, including liver (Cassiman et al., 2001; Passino et al., 2007), WAT (Baeza-Raja et al., 2012; Peeraully et al., 2004), and skeletal muscle (Deponti et al., 2009), but we do not know whether it affects obesity. p75^{NTR} expression increased in WAT after three weeks of HFD, but not in skeletal muscle or liver (Figure 1A). p75^{NTR} was also highly expressed in differentiated 3T3L1 and adipocytes derived from mouse embryonic fibroblast (MEF)-derived adipocytes (Figure S1A). To evaluate whether p75^{NTR} affects obesity, *p75^{NTR}*^{-/-} mice were placed on HFD and compared to their wild-type (WT) littermates. Interestingly, *p75^{NTR}*^{-/-} mice were resistant

to weight gain and remained lean after several weeks on HFD compared to controls (Figures 1B and S1B). $p75^{NTR-/-}$ mice also showed reduced adiposity, fat volume, and total weight of inguinal and intraperitoneal fat pads (Figures 1C and 1D). Weight did not differ between $p75^{NTR+/-}$ and WT mice on HFD (Figure S1C). Adipocytes were four-fold larger in control than $p75^{NTR-/-}$ fat pads from mice on HFD (Figures S1D and S1E). After just 3-weeks on HFD, adipocytes in WT mice were enlarged, while epididymal fat from $p75^{NTR-/-}$ mice contained smaller adipocytes (Figure S1E).

Obesity is a key trigger for type 2 diabetes, so we explored if $p75^{NTR-/-}$ mice are protected from insulin resistance. Basal insulin levels were three-fold higher in WT than $p75^{NTR-/-}$ mice on HFD (Figure 1E). $p75^{NTR-/-}$ mice also displayed increased insulin sensitivity, markedly improved glucose tolerance, and enhanced glucose lowering effects of insulin (Figures 1F, 1G, and S1F). With the hyperinsulinemic-euglycemic clamp technique, we found that glucose infusion rates were higher in $p75^{NTR-/-}$ mice than WT mice on HFD (Figure 1H), demonstrating improved systemic insulin sensitivity. Further, tracer-derived Rd or glucose disposal rate (GDR) and insulin-stimulated GDR were higher in $p75^{NTR-/-}$ mice (Figure 1I), indicating increased muscle insulin sensitivity. Basal hepatic glucose production (HGP) did not change in $p75^{NTR-/-}$ mice, but insulin-induced suppression of HGP increased from 40% to 64% (Figures S1G and S1H), showing decreased hepatic insulin resistance induced by HFD.

HFD triggers non-alcoholic fatty liver disease, which can cause liver steatosis, cirrhosis, and hepatocellular cancer (Osterreicher and Brenner, 2007). After 16 weeks of HFD, control mice developed and massively accumulated hepatic lipids and had increased liver weight, as expected, while $p75^{NTR-/-}$ mice were protected (Figures 1J and S2A). Livers from $p75^{NTR-/-}$ mice on HFD did not have higher levels of Sterol Regulatory Element-Binding Protein 1 (SREBP-1) (Figure S2B), a transcription factor that drives lipogenesis and molecularly marks liver steatosis (Shimomura et al., 1999). Liver triglycerides, SREBP-1 target genes, fatty acid-uptake genes, and fatty acid-oxidation genes were reduced in $p75^{NTR-/-}$ mice compared to WT mice on HFD (Figures S2C and S2D). Moreover, $p75^{NTR-/-}$ mice were protected from increased cholesterol and HFD-induced inflammation in WAT (Figures S2E and S2F). These results demonstrate that loss of $p75^{NTR}$ protects against obesity and the metabolic syndrome.

Loss of $p75^{NTR}$ Increases Energy Expenditure and Fat Oxidation

Food consumption and energy intake normalized to lean mass were similar in WT and $p75^{NTR-/-}$ mice (Figure 2A), suggesting that the lean phenotype of $p75^{NTR-/-}$ mice might be due to changes in energy expenditure and not appetite. Indeed, total oxygen consumption and energy expenditure were dramatically increased in $p75^{NTR-/-}$ compared to WT mice (Figure 2B), despite similar activity levels (Figure S3A). CO_2 production was also greater in $p75^{NTR-/-}$ mice (Figure S3B). Increased energy expenditure was confined to fat oxidation (Figures 2C and S3C).

Given that WAT regulates systemic energy (Rosen and Spiegelman, 2014), we analyzed fat oxidation and thermogenesis in adipocytes. Isolated adipocytes from $p75^{NTR-/-}$ mice had 2.4-fold higher fat oxidation than those from WT mice (Figure 2D), and 3-fold and 4-fold

higher uncoupling protein 1 (Ucp1) and deiodonase-2 (Dio2) expression, respectively (Figure 2E). Peroxisome proliferator-activated receptor δ (Ppar δ) and γ (Ppar γ) and *Ucp2* were unaffected (data not shown). Ucp1 protein and RNA, Ppar δ coactivator-1 α (Pgc-1 α), and Ppar α gene expression were increased in *p75^{NTR}-/-* WAT (Figures S3D and S3E). After cold exposure, core body temperatures were elevated in *p75^{NTR}-/-* mice (Figure S3F). Adiponectin, an adipocyte-derived hormone that increases fat oxidation (Fruebis et al., 2001) and correlates inversely with insulin resistance (Kadowaki et al., 2006), was higher in serum from *p75^{NTR}-/-* mice after HFD (Figure 2F). These results are consistent with increased fat oxidation in *p75^{NTR}-/-* adipocytes (Figure 2C) and insulin sensitivity in *p75^{NTR}-/-* mice (Figures 1E–1I and S1F–S1H). Adipocytes differentiation markers and lipid accumulation were similar between WT and *p75^{NTR}-/-* adipocytes (Figures S4A and S4B), suggesting that decreased adipogenesis was not due to impaired adipocyte differentiation in *p75^{NTR}-/-* mice. Decreased adipogenesis was also not due to altered lipogenesis capacity, as expression of lipogenic genes, including fatty acid synthase (Fas) and diglyceride acyl-transferase-1 (Dgat1), were not affected (Figure S4C). In brown adipose tissue (BAT), *p75^{NTR}* expression did not increase with HFD (Figure S4D). Expression of thermogenic genes, fat oxidation, and molecular markers for brown adipocytes were also not different between BAT from WT and *p75^{NTR}-/-* mice on HFD (Figure S4E), suggesting that increased energy expenditure was not due to *p75^{NTR}* expression in BAT. These data indicate that loss of *p75^{NTR}* promotes fat oxidation and energy expenditure in WAT.

***p75^{NTR}* Depletion Increases Adipocyte Lipolysis by Regulating the cAMP/PKA Signaling Pathway**

Increased lipolysis in WAT without release of circulating free fatty acids (FFAs) promotes energy dissipation and fat oxidation and protects against HFD-induced obesity (Ahmadian et al., 2009). We examined if lipolysis decreased adiposity in *p75^{NTR}-/-* mice and increased energy expenditure and fat oxidation in *p75^{NTR}-/-* adipocytes. While basal rates were unchanged (Figure S5A), FFA and glycerol release were higher in WAT explants and MEF-derived adipocytes from *p75^{NTR}-/-* mice after isoproterenol stimulation (Figures 3A, S5B, and S5C), while circulating FFA levels were unaffected in *p75^{NTR}-/-* mice on HFD (Figure S5D). Isoproterenol increased FFA release by 1.6-fold and 2.5-fold in WT and *p75^{NTR}-/-* WAT, respectively (Figure S5B), similar to prior studies (Jaworski et al., 2009). Neurotrophins did not affect FFA secretion in WT or *p75^{NTR}-/-* WAT (Figure S5E), suggesting that lipolysis is a neurotrophin-independent function.

Signaling through the cAMP/Protein Kinase A (PKA) pathway primarily regulates lipolysis (Zechner et al., 2012). We found that lipolysis and cAMP levels were significantly higher in *p75^{NTR}-/-* compared to WT WAT on HFD (Figures 3A and 3B) but not on normal chow (Figures 3B and S5F). Inhibiting PKA with H-89 decreased FFA release in *p75^{NTR}-/-* WAT (Figure 3C), indicating that cAMP/PKA signaling is required for increased lipolysis in *p75^{NTR}-/-* WAT. cAMP/PKA signaling promotes lipolysis in WAT via PKA-mediated phosphorylation of hormone-sensitive lipase (HSL) (Haemmerle et al., 2002; Osuga et al., 2000). We found that phosphorylated HSL (P-HSL) was increased in *p75^{NTR}-/-* WAT and MEF-derived adipocytes (Figures 3D and S5G). Hsl gene expression was increased by ~1.8-fold (Figure S5H), but HSL protein was not significantly increased in *p75^{NTR}-/-* WAT

(Figure 3D) and MEF-derived adipocytes (Figure S5G). Phosphorylation of other PKA targets, including perilipin, cAMP response element-binding protein (CREB) (P-CREB), and p38 (P-p38), were also increased in *p75^{NTR}-/-* WAT (Figure 3D) and MEF-derived adipocytes (Figure S5G). These results support that p75^{NTR} regulates lipolysis by modulating cAMP/PKA signaling and catecholamine sensitivity.

p75^{NTR} Directly Binds the Regulatory and Catalytic PKA Subunits and Regulates PKA Holoenzyme Dissociation

Dissociation of the PKA subunits is a critical step for PKA activation (Taylor et al., 2012). To explore how p75^{NTR} regulates cAMP/PKA signaling, we examined if p75^{NTR} regulates the tetrameric PKA holoenzyme by studying the interaction between the catalytic (C α) and regulatory (RII β) PKA subunits. Intriguingly, the C α subunit was dissociated from RII β in *p75^{NTR}-/-* MEF-derived adipocytes (Figure 3E), despite no differences in protein expression of PKA subunits (Figure 3F). These results indicate that p75^{NTR} deletion causes constitutive dissociation and activation of the PKA catalytic subunit, which agrees with increased cAMP levels (Figure 3B), lipolysis (Figures 3A, S5B), and HSL phosphorylation (Figures 3D and S5G) in *p75^{NTR}-/-* adipocytes. p75^{NTR} bound both C α and RII β when co-immunoprecipitated from overexpression systems (Figure 3G) and endogenously in WAT (Figure 3H). In binding assays, the intracellular domain of p75^{NTR} (p75ICD) directly interacted with both C α and RII β , but not with the unrelated protein Hsp20 (Figure 3I). Screening an array library of overlapping p75ICD 25-mer peptides revealed that C α and RII β bound within helix 5 (peptides 16–21, aa 348–397) and 6 (peptides 23–25, aa 383–417) of the death domain (DD) of p75ICD, respectively (Figure 4A). An alanine scanning substitution array of p75ICD identified key residues that enable its interaction with C α as C379 and RII β as P380, R382, L385, R404, R405, and R408 (Figures 4B and 4C). Thus, we performed site-specific mutagenesis of p75^{NTR} (Figure 4D) and found that the C379A mutation abolished its interaction with C α , while mutations of the other residues for RII β abolished its interaction with RII β (Figures 4E and 4F). These results support that p75^{NTR} directly interacts with PKA subunits through motifs within its DD.

Next, we tested in adipocytes the interaction of p75^{NTR} with cAMP-degrading phosphodiesterases (PDEs) and the functional consequences of p75^{NTR} mutants that disrupt the interaction of p75^{NTR} with PKA subunits. Consistent with our prior study (Sachs et al., 2007), p75^{NTR} co-immunoprecipitated with cAMP-hydrolyzing enzyme phosphodiesterase 4A5 (PDE4A5) in WAT and adipocytes (Figure S6A). Lentiviral expression of WT p75^{NTR} or p75^{NTR}C379A reduced P-HSL levels in *p75^{NTR}-/-* MEF-derived adipocytes by ~2-fold and ~1.5-fold, respectively (Figure 4G). Expression of the p75^{NTR}2M mutant, which reduces binding of p75^{NTR} to PKA-RII β , did not alter P-HSL (Figure 4G). We performed these analyses with isoproterenol (Figure 4G), because at baseline, control lentivirus increased basal levels of P-HSL (Figure S6B). Lentiviral expression of both WT p75^{NTR} and p75^{NTR}C379A reduced cAMP levels (Figure S6C), suggesting that p75^{NTR} regulates cAMP/PKA signaling through multiple pathways.

Adipocyte-specific p75^{NTR} Knockout Protects from HFD-Induced Obesity and Insulin Resistance

To investigate how adipose tissue contributes to the lean phenotype and insulin sensitivity of *p75^{NTR}-/-* mice on a HFD, we knocked out p75^{NTR} specifically in adipocytes (*p75^{AKO}*) using conditional *p75^{NTR}* knockout (*p75^{F/F}*) (Bogenmann et al., 2011) and *aP2-cre* (*Adipocyte-cre*) mice that show gene recombination specifically in adipocytes without gene recombination in brain, muscle, liver, stromal vascular cells, and macrophages (Ahmadian et al., 2011; Barak et al., 2002; He et al., 2003; Lee et al., 2014; Li et al., 2011; Paschos et al., 2012; Qi et al., 2009). In *p75^{AKO}* mice, p75^{NTR} was specifically deleted in adipose tissue and not the brain and muscle (Figures 5A and 5B). Strikingly, *p75^{AKO}* mice weighed significantly less (Figure 5C) and showed improved glucose and insulin tolerance (Figure 5D), suggesting that specifically deleting p75^{NTR} from adipose tissue protects against diet-induced obesity and type 2 diabetes. In addition, livers from *p75^{AKO}* mice on HFD showed reduced SREBP-1 and hepatic lipid accumulation compared to WT mice (Figures S7A and S7B). In contrast, muscle-specific knockout mice (*p75^{MKO}*) had similar weight gain to *p75^{F/F}* and *muscle creatine kinase (MCK)-cre* control mice (Figures 5E and 5F). These results support the reduced body weight gain and increased insulin sensitivity in *p75^{NTR}-/-* mice after HFD, demonstrating that deleting p75^{NTR} from adipocytes protects against HFD-induced obesity and insulin resistance. *p75^{AKO}* mice showed increased energy expenditure and fat oxidation, despite similar activity and no changes in food consumption and energy intake (Figures 6A-6C and S7C-S7E), similar to *p75^{NTR}-/-* mice on HFD (Figures 2 and S3A-C). WAT isolated from *p75^{AKO}* mice showed increased metabolic rates via increased expression of thermogenic, brown adipose identity, and lipolytic genes such as *Dio2*, *Ucp-1*, *Pgc-1 α* , *Ppara α* , and *Hsl* (Figure 6D). HSL phosphorylation was also increased in WAT of *p75^{AKO}* compared to control mice (Figure 6E). These results indicate that adipose-specific expression of p75^{NTR} is a major contributor to obesity, energy expenditure, and lipolysis.

To further analyze the adipose-specific role of p75^{NTR} *in vivo*, we transplanted epididymal fat pads from *p75^{NTR}-/-* mice into the visceral area of WT (*p75^{NTR}-/-*→WT) mice (Figure 7A). After 6 weeks on HFD, the increase in body weight was significantly lower in *p75^{NTR}-/-*→WT compared to WT→WT WAT or sham operated controls (Figure 7B). *p75^{NTR}-/-*→WT mice also showed improved glucose and insulin tolerance 10 weeks after HFD (Figure 7C). Insulin sensitivity was unaffected in WT→WT or sham operated mice (Figure 7C), as expected (Tran et al., 2008). The effect of *p75^{NTR}-/-* WAT transplantation on body weight and insulin sensitivity on WT mice is significant and the values obtained are at similar range observed in other transplant studies (Chen et al., 2003; Minamino et al., 2009). WT→*p75^{NTR}-/-* mice remained lean and insulin-sensitive upon HFD (Figures 7D-7F), likely because they retained a substantial amount of *p75^{NTR}-/-* fat. These results indicate that p75^{NTR} expression in WAT regulates fat oxidation, thermogenesis, lipolysis, and HFD-induced weight gain and insulin resistance in mice.

Discussion

Many studies have addressed the key mechanisms in adipocytes that regulate energy balance, but the molecular links between diet, energy storage and mobilization, and

mutation(s) that selectively inhibit the interaction between p75^{NTR} and PKA in vivo may reveal the relative contribution of p75^{NTR} signal transduction pathways in metabolic diseases and other biological function within and outside of the nervous system.

p75^{NTR} interacts with both PKA and PDEs, and PKA works with PDEs to create a signaling complex or “signalosome” (Taylor et al., 2012). Similar to p75^{NTR}, A-kinase anchoring proteins (AKAPs) directly bind PKA and PDEs to compartmentalize cAMP/PKA signaling by associating with target effectors, substrates, and signal termination (Baillie et al., 2005; Carr et al., 1991; Dodge-Kafka et al., 2005). Canonical AKAPs are characterized by the specific amphipathic helix of 14–18 aa that bind PKA subunits (McConnachie et al., 2006). Although p75^{NTR} does not contain the AKAP amphipathic helix, p75^{NTR} might function as a non-conventional AKAP-regulating PKA signal by directly binding both PKA subunits and PDEs. Moreover, given that regulation of PKA is critical in metabolism and neuronal functions, p75^{NTR} might regulate cAMP/PKA signaling in neuronal cells (Zhong et al., 2009). Structural biology studies are needed to understand the PKA holoenzymes and macromolecular assemblies that regulate cAMP/PKA signaling (Kim et al., 2007; Zhang et al., 2012). These studies will determine the contribution of a potential PDE4A-p75^{NTR}-PKA macromolecular complex in cAMP regulation and will characterize the properties of p75^{NTR} as a “non-conventional” AKAP in peripheral tissues and the brain.

p75^{NTR}^{-/-} mice were protected against HFD-induced insulin resistance through significantly enhanced insulin sensitivity in skeletal muscle, hepatic, and adipose tissue. Since *p75^{NTR}^{-/-}* mice remain lean on *HFD* their resistance to type 2 diabetes could be a secondary effect to reduced body weight. Increased insulin sensitivity in *p75^{NTR}^{-/-}* mice on normal chow (Baeza-Raja et al., 2012) might also contribute to reduced insulin resistance upon HFD. *p75^{AKO}* mice and *p75^{NTR}^{-/-}→WT* mice showed increased systemic insulin sensitivity after HFD, emphasizing the primacy of WAT in systemic insulin regulation and its communication with other key metabolic organs to enhance insulin sensitivity. In this regard, *p75^{NTR}^{-/-}* mice showed substantial increases in circulating levels of adiponectin, an adipocyte-derived hormone that reduces insulin resistance and liver steatosis by increasing fat oxidation via the AMP-activated protein kinase pathway (Fruebis et al., 2001; Xu et al., 2003a). Increased lipolysis induces fatty acid oxidation. Thus, potential increases in oxidation could also be interpreted as consequences of increased lipolysis. For example, reciprocal regulation of lipolysis and fat oxidation associated with crosstalk between the cAMP/PKA pathway and Sirt-1 regulates fatty acid oxidation (Gerhart-Hines et al., 2011). Our study shows that p75^{NTR} does not regulate adipocyte differentiation, which supports prior studies showing that defects in lipolysis do not affect adipocyte differentiation. For example, similar to *p75^{NTR}^{-/-}* mice, AdPLA knock-out adipocytes showed normal intracellular lipid accumulation and significantly increased lipolysis (Jaworski et al., 2009). Regulation of lipolysis without effects in adipocyte differentiation suggests that lipolysis is a primary effect of p75^{NTR}. *p75^{NTR}^{-/-}* mice show increased lipolytic rates without increasing serum FA, suggesting that increased fatty acid oxidation protects *p75^{NTR}^{-/-}* mice from increased lipolysis. Indeed, adipocytes can increase FFA use and energy expenditure without increasing serum FA levels (Ahmadian et al., 2009). Thus, weight reduction and increased lipid oxidation might be due, in part, to increased synthesis of adiponectin or other adipokines or metabolites derived from WAT. While glucose tolerance significantly

improved in $p75^{AKO}$ and $p75^{NTR-/-} \rightarrow WT$ mice 8 weeks after HFD it was reduced compared to $p75^{NTR-/-}$ mice tested 20 weeks after HFD. These differences may be due to effects of $p75^{NTR}$ expression in tissues other than adipose tissue or to different time points used to measure glucose tolerance.

Our study shows increased P-HSL in WAT isolated from $p75^{NTR-/-}$ (Figure 3D) and $p75^{AKO}$ mice (Figure 6E), and in $p75^{NTR-/-}$ MEF-derived adipocytes cultured in vitro (Figure S5G), indicating that $p75^{NTR}$ loss similarly increases P-HSL in WAT and MEF-derived adipocytes. As expected, the relative fold-changes are different between tissue isolated from mice (Figure 3D) and cultured cells (Figure S5G). The ~ 1.8 -fold and ~ 2.3 -fold increases in *Hsl* RNA in $p75^{NTR-/-}$ WAT (Figure S5H) and $p75^{AKO}$ mice (Figure 6D), respectively, did not change total HSL protein. These results further suggest that $p75^{NTR}$ contributes to PKA-mediated phosphorylation of HSL (Figures 3D and 6E). These results are consistent with prior studies showing that HSL is primarily regulated post-translationally (Kraemer and Shen, 2002). We also found a ~ 7 -fold and ~ 2.5 -fold increase in P-HSL in WAT isolated from $p75^{AKO}$ and control *Adipocyte-Cre* mice, respectively. Since phosphorylation of HSL in vivo depends on fasting conditions (Kraemer and Shen, 2002), variability in P-HSL within animals may be due to their responses to fasting. Regardless of the expected variability of signal transduction in vivo, the increase in P-HSL in $p75^{AKO}$ mice supports the data obtained in vivo in $p75^{NTR-/-}$ mice and *in vitro* in $p75^{NTR-/-}$ MEF-derived adipocytes showing that $p75^{NTR}$ depletion in fat increases HSL phosphorylation. We also evaluated PKA-mediated phosphorylation of perilipin by pulling down perilipin and blotting with P-PKA (Choi et al., 2010; Marcinkiewicz et al., 2006). Our study tested phosphorylation of all six potential PKA phosphorylation sites on perilipin (Greenberg et al., 1993; Zhang et al., 2003) by pulling-down perilipin and blotting with anti-P-PKA. Future studies will map the potential specific phosphorylation sites of perilipin that are regulated by $p75^{NTR}$.

While $p75^{NTR}$ is expressed in all tissues involved in metabolic regulation, our genetic and transplantation studies support that WAT is the primary site of action for $p75^{NTR}$. Similar to $p75^{NTR-/-}$ mice, specifically deleting $p75^{NTR}$ from adipocytes also protected against HFD-induced obesity, while specifically deleting it from muscle did not. Further, primary cultures of $p75^{NTR-/-}$ adipocytes had dramatically increased lipolysis, fat oxidation, and thermogenesis. Moreover, $p75^{NTR-/-} \rightarrow WT$ mice were protected from increased body weight after HFD. Although these studies cannot exclude the potential effect of secreted factors by WAT, they strongly support that deleting $p75^{NTR}$ from adipocytes has beneficial metabolic effects. $p75^{NTR}$ was upregulated in WAT after exposure to HFD. Although transcription factors, such as CLOCK/BMAL, regulate $p75^{NTR}$ expression (Baeza-Raja et al., 2013), the transcriptional mechanisms that control its upregulation after injury or disease remain unknown. Thus, proinflammatory signals might increase $p75^{NTR}$ levels in WAT upon HFD. These results suggest that adipose tissue is a primary site for $p75^{NTR}$ to functionally regulate body weight, insulin resistance, lipolysis, and energy expenditure. Future studies will explore the potential contribution of $p75^{NTR}$ expression in other tissues, such as the nervous system, liver, skeletal muscle, macrophages, and BAT to its metabolic functions.

Our data show that HFD increases p75^{NTR} expression. In accordance with our prior work (Sachs et al., 2007), cAMP/PKA signaling is inhibited in p75^{NTR}-expressing cells. Several signaling pathways are activated after ligands bind to p75^{NTR}; however, p75^{NTR} also contributes to many signaling pathways and biological functions independent of ligands (Barker, 2004; Teng and Hempstead, 2004; Zampieri and Chao, 2006). For example, p75^{NTR} can serve as a co-receptor for receptors other than neurotrophins, such as the Nogo receptor and ephrin-As (Domeniconi et al., 2005; Lim et al., 2008; Wong et al., 2002). p75^{NTR} can also induce signaling independent of neurotrophins and/or the function of a co-receptor. Prior studies suggested that p75^{NTR} may signal in a neurotrophin-independent manner in neuronal cells to induce apoptosis (Majdan et al., 1997; Rabizadeh et al., 1993) and activate PI3 Kinase (Roux et al., 2001), RhoA (Yamashita et al., 1999), PDE4A (Sachs et al., 2007), hypoxia inducible factor (HIF)-1 α (Le Moan et al., 2011), and transforming growth factor (TGF)- β (Schachtrup et al., 2015). In these studies, expressing p75^{NTR} alone could exert a signaling event and biological effect without a neurotrophin ligand. Moreover, crosslinking of p75^{NTR} dimers constitutively activates several pathways independent of ligands (Vilar et al., 2009). Since p75^{NTR} is not constitutively expressed, but is upregulated upon HFD, its expression could trigger activation of a signaling pathway. Since tumor necrosis factor (TNF)- α and interleukin (IL)-1 β induce p75^{NTR} expression, increased pro-inflammatory activity upon HFD might augment p75^{NTR} levels (Choi and Friedman, 2009). There are several examples of well-established ligand-independent signaling pathways in other receptor systems. For example, steroid hormone receptors (Power et al., 1991), scavenger receptors (Li et al., 2005), viral G-protein-coupled receptors (Vischer et al., 2006), androgen receptors (Culig, 2004), and B-cell receptors (Monroe, 2004) all signal in a ligand-independent manner. Future studies will address the potential endogenous mechanisms that might modulate increased expression of p75^{NTR} upon HFD.

In prior studies, *p75^{NTR}-/-* mice have shown many physiological phenotypes, including deficits in sensory nerve development (Lee et al., 1994), neurogenesis (Young et al., 2007; Zuccaro et al., 2014), and insulin resistance (Baeza-Raja et al., 2012). *p75^{NTR}-/-* mice have also shown many pathological phenotypes, such as deficits in oligodendrocyte apoptosis (Beattie et al., 2002), liver regeneration (Passino et al., 2007), retinal hypoxia (Le Moan et al., 2011), and astrocyte functions (Schachtrup et al., 2015). Our study identified a fundamental role for p75^{NTR} in metabolism given the dramatic resistance of *p75^{NTR}-/-* mice to diet-induced obesity. Proteins like p75^{NTR}, which are expressed in several tissues and control multiple signaling pathways, commonly have pleiotropic biological functions in vivo. For example, many phenotypes have been seen in the brain and peripheral tissues of mice depleted of transcription factors like NF- κ B and Sirt-1, or scaffold proteins like β -arrestin. We have shown that *p75^{NTR}-/-* mice have reduced HIF-1 α and are resistant to hypoxia (Le Moan et al., 2011). Indeed, fat-specific depletion of HIF-1 α improves insulin sensitivity and decreases adiposity in HFD-fed mice (Jiang et al., 2011). Since *p75^{NTR}-/-* mice have reduced HIF-1 α only after exposure to hypoxic conditions, local tissue hypoxia in fat might decrease HIF-1 α in *p75^{NTR}-/-* fat after HFD. This mechanism would support our model, since both fat-specific depletion of HIF-1 α and *p75^{NTR}-/-* mice show similar phenotypes upon diet-induced obesity. We have also shown that *p75^{NTR}-/-* mice had no significant differences in circadian rhythms in vivo (Baeza-Raja et al., 2013), suggesting that

circadian regulation is unlikely to affect the metabolic phenotype of the $p75^{NTR-/-}$ mice. The dramatic biological effect of $p75^{NTR}$ in obesity suggests that metabolic regulation could be one of the most critical in vivo functions for $p75^{NTR}$. Further, $p75^{NTR-/-}$ mice on HFD could be a novel experimental model to study mechanisms of obesity and energy balance.

In summary, this study demonstrates that the obesity-dependent induction of $p75^{NTR}$ in WAT represses lipolysis and energy expenditure by directly binding and regulating the PKA holoenzyme dissociation, thus majorly contributing to the generation of obesity. By developing agents that target the $p75^{NTR}$ ICD in the periphery, we may discover attractive therapeutic strategies to increase energy expenditure and prevent obesity, liver steatosis, and diabetes.

Experimental Procedures

Animals

Wild-type (WT), $p75^{NTR-/-}$ (Lee et al., 1992), *adipo-cre* (*AP2-cre*) (He et al., 2003), and *MCK-cre* (Bruning et al., 1998) mice were in a C57BL/6J background (The Jackson Laboratory). Heterozygous $p75^{NTR+/-}$ mice were crossed to obtain $p75^{NTR-/-}$, $p75^{NTR+/-}$ and $p75^{NTR+/+}$ littermates. $p75^{NTRflox/flox}$ ($p75^{F/F}$) (Bogenmann et al., 2011) mice in the C57BL/6J background were also used. Crossings between $p75^{F/F}$ and *Adipocyte-cre*, or *MCK-cre* were performed to generate $p75^{AKO}$ (*AP2-cre*: $p75^{NTRflox/flox}$) or $p75^{MKO}$ (*MCK-cre*: $p75^{NTRflox/flox}$) mice. Male mice 9–25-weeks-old were used. Mice were housed under a 12 h light/dark cycle, fed a standard chow or high-fat diet (HFD) (60% calories from fat, D12492, research diets), and had access to food and water *ad libitum*. All animal experiments were performed under the guidelines set by the Institutional Animal Care and Use Committee of the University of California San Francisco and San Diego and are in accordance with the National Institutes of Health.

Metabolic cages

The Comprehensive Lab Animal Monitoring Systems (Columbus Instruments) was used to measure food intake, movement, volume of carbon dioxide produced (VCO_2), volume of oxygen consumed (VO_2), respiration rate ($RER = VCO_2/VO_2$), and caloric output $[(3.815 + 1.232 \times RER) \times VO_2]$ over 5 consecutive days. Mice were housed in individual cages for 5 days and allowed to acclimate in the recording metabolic chambers for 24 hours before the start of measurements to minimize stress. Mouse weights and body composition were determined before the monitoring period. Body composition was determined by quantitative magnetic resonance on the EchoMRI-3in1 body composition analyzer (EchoMRI). Fat and lean mass were determined by the system software. Data were normalized to body weights except VO_2 and VCO_2 , which were normalized to lean mass. Fat oxidation was calculated using the formula $((1.695 \times VO_2) - (1.701 \times VCO_2)) \times 9$. Values were normalized by lean mass. Measurements of energy intake and energy expenditure were averaged over 4 light and dark periods.

Co-immunoprecipitation

Co-IP was performed as described previously (Le Moan et al., 2011). Cell lysates were prepared in 1% NP-40, 200 mM NaCl, 1 mM EDTA, and 20 mM Tris-HCl, pH 8.0. Rabbit anti-p75^{NTR} antibody 9992 (kind gift of Moses Chao), rabbit anti-PKAC α (Cell Signaling), and rabbit anti-perilipin (Cell Signaling) were used for IP, and immunoblots were performed with anti-PKAC α , anti-PKARII α , anti-PKARII β , anti-PDE4A, anti-phospho PKA substrate, and anti-p75^{NTR}. Additionally, rabbit anti-HA and mouse anti-Myc were used for IP, and immunoblots were performed with anti-GFP, anti-HA, and anti-Myc.

cAMP, active PKA, adiponectin, triglycerides, and cholesterol

cAMP (Assay Designs) and active PKA (Enzo Life sciences) were measured following manufacturer's instructions. Forskolin (10 μ M; Sigma) was added for 1 hour. Adiponectin in serum was measured by ELISA (Bbridge International) according to manufacturer's instructions. Liver triglycerides (Abcam) were measured following manufacturer's instructions. Total blood cholesterol was measured using PTS Panels test strips (Polymer Technology Systems, Inc.) on blood samples collected from animals after fasting.

Statistical analysis

Statistical significance was calculated with GraphPad Prism (GraphPad Prism Software) by unpaired two-sided Student's *t*-test to analyze significance between two experimental groups, by non-parametric two-sided Mann-Whitney test, Tukey's multiple-comparisons test, one-way ANOVA, or two-way ANOVA for multiple comparisons followed by a Bonferroni's post-test. Data are shown as the means \pm SEM.

Supplementary Material

Refer to Web version on PubMed Central for supplementary material.

Acknowledgments

We thank Moses V. Chao for providing reagents and helpful discussions; Matthew D. Hirschey and Carrie A. Grueter for providing reagents and technical support; Jody L. Baron and Anthony Wynshaw-Boris for advice; Margo Streets, Dennis Young, Rima Boyadjian, Belinda Cabriga, and Peter Tontonoz for technical support; and Ruth MacLeod and Jane E. Findlay for peptide array synthesis. F.C. and G.S.B. were supported by Grant MRC G0600765 and J007412 from the Medical Research Council (UK). B.D.S was supported by the NIH/NINDS, Ruth L. Kirschstein National Research Service Awards for Individual Predoctoral Fellowship and B.B-R. was supported by the Spanish Research Foundation for postdoctoral fellowship. We thank Vesa Kaartinen for providing us with the p75^{NTR} conditional mice. S.S.T. was supported by NIH grant DK054441. K.A. was supported by grants from the UCSF Liver Center (P30 DK026743) and Diabetes and Endocrinology Center (P30 DK63720) and NIH/NINDS grant NS051470. K.A. conceived the project, designed the study, analyzed and interpreted data.

References

- Ahmadian M, Abbott MJ, Tang T, Hudak CS, Kim Y, Bruss M, Hellerstein MK, Lee HY, Samuel VT, Shulman GI, Wang Y, Duncan RE, Kang C, Sul HS. Desnutrin/ATGL is regulated by AMPK and is required for a brown adipose phenotype. *Cell Metab.* 2011; 13:739–748. [PubMed: 21641555]
- Ahmadian M, Duncan RE, Sul HS. The skinny on fat: lipolysis and fatty acid utilization in adipocytes. *Trends Endocrinol Metab.* 2009; 20:424–428. [PubMed: 19796963]

- Baeza-Raja B, Eckel-Mahan K, Zhang L, Vagena E, Tsigelny IF, Sassone-Corsi P, Ptacek LJ, Akassoglou K. p75 neurotrophin receptor is a clock gene that regulates oscillatory components of circadian and metabolic networks. *J Neurosci*. 2013; 33:10221–10234. [PubMed: 23785138]
- Baeza-Raja B, Li P, Le Moan N, Sachs BD, Schachtrup C, Davalos D, Vagena E, Bridges D, Kim C, Saitiel AR, Olefsky JM, Akassoglou K. p75 neurotrophin receptor regulates glucose homeostasis and insulin sensitivity. *Proc Natl Acad Sci U S A*. 2012; 109:5838–5843. [PubMed: 22460790]
- Baillie GS, Scott JD, Houslay MD. Compartmentalisation of phosphodiesterases and protein kinase A: opposites attract. *FEBS Lett*. 2005; 579:3264–3270. [PubMed: 15943971]
- Barak Y, Liao D, He W, Ong ES, Nelson MC, Olefsky JM, Boland R, Evans RM. Effects of peroxisome proliferator-activated receptor delta on placentation, adiposity, and colorectal cancer. *Proc Natl Acad Sci U S A*. 2002; 99:303–308. [PubMed: 11756685]
- Barker PA. p75NTR is positively promiscuous: novel partners and new insights. *Neuron*. 2004; 42:529–533. [PubMed: 15157416]
- Beattie MS, Harrington AW, Lee R, Kim JY, Boyce SL, Longo FM, Bresnahan JC, Hempstead BL, Yoon SO. ProNGF induces p75-mediated death of oligodendrocytes following spinal cord injury. *Neuron*. 2002; 36:375–386. [PubMed: 12408842]
- Bogenmann E, Thomas PS, Li Q, Kim J, Yang LT, Pierchala B, Kaartinen V. Generation of mice with a conditional allele for the p75(NTR) neurotrophin receptor gene. *Genesis*. 2011; 49:862–869. [PubMed: 21413144]
- Bruning JC, Michael MD, Winnay JN, Hayashi T, Horsch D, Accili D, Goodyear LJ, Kahn CR. A muscle-specific insulin receptor knockout exhibits features of the metabolic syndrome of NIDDM without altering glucose tolerance. *Mol Cell*. 1998; 2:559–569. [PubMed: 9844629]
- Carr DW, Stofko-Hahn RE, Fraser ID, Bishop SM, Acott TS, Brennan RG, Scott JD. Interaction of the regulatory subunit (RII) of cAMP-dependent protein kinase with RII-anchoring proteins occurs through an amphipathic helix binding motif. *J Biol Chem*. 1991; 266:14188–14192. [PubMed: 1860836]
- Cassiman D, Deneff C, Desmet VJ, Roskams T. Human and rat hepatic stellate cells express neurotrophins and neurotrophin receptors. *Hepatology*. 2001; 33:148–158. [PubMed: 11124831]
- Chen HC, Jensen DR, Myers HM, Eckel RH, Farese RV Jr. Obesity resistance and enhanced glucose metabolism in mice transplanted with white adipose tissue lacking acyl CoA:diacylglycerol acyltransferase 1. *J Clin Invest*. 2003; 111:1715–1722. [PubMed: 12782674]
- Choi S, Friedman WJ. Inflammatory cytokines IL-1beta and TNF-alpha regulate p75NTR expression in CNS neurons and astrocytes by distinct cell-type-specific signalling mechanisms. *ASN Neuro*. 2009; 1
- Choi SM, Tucker DF, Gross DN, Easton RM, DiPilato LM, Dean AS, Monks BR, Birnbaum MJ. Insulin regulates adipocyte lipolysis via an Akt-independent signaling pathway. *Mol Cell Biol*. 2010; 30:5009–5020. [PubMed: 20733001]
- Culig Z. Androgen receptor cross-talk with cell signalling pathways. *Growth Factors*. 2004; 22:179–184. [PubMed: 15518241]
- Cummings DE, Brandon EP, Planas JV, Motamed K, Idzerda RL, McKnight GS. Genetically lean mice result from targeted disruption of the RII beta subunit of protein kinase A. *Nature*. 1996; 382:622–626. [PubMed: 8757131]
- Deponti D, Buono R, Catanzaro G, De Palma C, Longhi R, Meneveri R, Bresolin N, Bassi MT, Cossu G, Clementi E, Brunelli S. The low-affinity receptor for neurotrophins p75NTR plays a key role for satellite cell function in muscle repair acting via RhoA. *Mol Biol Cell*. 2009; 20:3620–3627. [PubMed: 19553472]
- Dodge-Kafka KL, Soughayer J, Pare GC, Carlisle Michel JJ, Langeberg LK, Kapiloff MS, Scott JD. The protein kinase A anchoring protein mAKAP coordinates two integrated cAMP effector pathways. *Nature*. 2005; 437:574–578. [PubMed: 16177794]
- Domeniconi M, Zampieri N, Spencer T, Hilaire M, Mellado W, Chao MV, Filbin MT. MAG induces regulated intramembrane proteolysis of the p75 neurotrophin receptor to inhibit neurite outgrowth. *Neuron*. 2005; 46:849–855. [PubMed: 15953414]
- Fruebis J, Tsao TS, Javorschi S, Ebbets-Reed D, Erickson MR, Yen FT, Bihain BE, Lodish HF. Proteolytic cleavage product of 30-kDa adipocyte complement-related protein increases fatty acid

- oxidation in muscle and causes weight loss in mice. *Proc Natl Acad Sci U S A*. 2001; 98:2005–2010. [PubMed: 11172066]
- Gerhart-Hines Z, Dominy JE Jr, Blattler SM, Jedrychowski MP, Banks AS, Lim JH, Chim H, Gygi SP, Puigserver P. The cAMP/PKA pathway rapidly activates SIRT1 to promote fatty acid oxidation independently of changes in NAD(+). *Mol Cell*. 2011; 44:851–863. [PubMed: 22195961]
- Greenberg AS, Egan JJ, Wek SA, Moos MC Jr, Londos C, Kimmel AR. Isolation of cDNAs for perilipins A and B: sequence and expression of lipid droplet-associated proteins of adipocytes. *Proc Natl Acad Sci U S A*. 1993; 90:12035–12039. [PubMed: 7505452]
- Haemmerle G, Zimmermann R, Hayn M, Theussl C, Waeg G, Wagner E, Sattler W, Magin TM, Wagner EF, Zechner R. Hormone-sensitive lipase deficiency in mice causes diglyceride accumulation in adipose tissue, muscle, and testis. *J Biol Chem*. 2002; 277:4806–4815. [PubMed: 11717312]
- He W, Barak Y, Hevener A, Olson P, Liao D, Le J, Nelson M, Ong E, Olefsky JM, Evans RM. Adipose-specific peroxisome proliferator-activated receptor gamma knockout causes insulin resistance in fat and liver but not in muscle. *Proc Natl Acad Sci U S A*. 2003; 100:15712–15717. [PubMed: 14660788]
- Iwami G, Kawabe J, Ebina T, Cannon PJ, Homcy CJ, Ishikawa Y. Regulation of adenylyl cyclase by protein kinase A. *J Biol Chem*. 1995; 270:12481–12484. [PubMed: 7759492]
- Jaworski K, Ahmadian M, Duncan RE, Sarkadi-Nagy E, Varady KA, Hellerstein MK, Lee HY, Samuel VT, Shulman GI, Kim KH, de Val S, Kang C, Sul HS. AdPLA ablation increases lipolysis and prevents obesity induced by high-fat feeding or leptin deficiency. *Nat Med*. 2009; 15:159–168. [PubMed: 19136964]
- Jiang C, Qu A, Matsubara T, Chanturiya T, Jou W, Gavrilova O, Shah YM, Gonzalez FJ. Disruption of hypoxia-inducible factor 1 in adipocytes improves insulin sensitivity and decreases adiposity in high-fat diet-fed mice. *Diabetes*. 2011; 60:2484–2495. [PubMed: 21873554]
- Kadowaki T, Yamauchi T, Kubota N, Hara K, Ueki K, Tobe K. Adiponectin and adiponectin receptors in insulin resistance, diabetes, and the metabolic syndrome. *J Clin Invest*. 2006; 116:1784–1792. [PubMed: 16823476]
- Kim C, Cheng CY, Saldanha SA, Taylor SS. PKA-I holoenzyme structure reveals a mechanism for cAMP-dependent activation. *Cell*. 2007; 130:1032–1043. [PubMed: 17889648]
- Kraemer FB, Shen WJ. Hormone-sensitive lipase: control of intracellular tri-(di-)acylglycerol and cholesteryl ester hydrolysis. *J Lipid Res*. 2002; 43:1585–1594. [PubMed: 12364542]
- Le Moan N, Houslay DM, Christian F, Houslay MD, Akassoglou K. Oxygen-dependent cleavage of the p75 neurotrophin receptor triggers stabilization of HIF-1alpha. *Mol Cell*. 2011; 44:476–490. [PubMed: 22055192]
- Lee KF, Davies AM, Jaenisch R. p75-deficient embryonic dorsal root sensory and neonatal sympathetic neurons display a decreased sensitivity to NGF. *Development*. 1994; 120:1027–1033. [PubMed: 7600951]
- Lee KF, Li E, Huber LJ, Landis SC, Sharpe AH, Chao MV, Jaenisch R. Targeted mutation of the gene encoding the low affinity NGF receptor p75 leads to deficits in the peripheral sensory nervous system. *Cell*. 1992; 69:737–749. [PubMed: 1317267]
- Lee YS, Kim JW, Osborne O, Oh DY, Sasik R, Schenk S, Chen A, Chung H, Murphy A, Watkins SM, Quehenberger O, Johnson RS, Olefsky JM. Increased Adipocyte O2 Consumption Triggers HIF-1α Causing Inflammation and Insulin Resistance in Obesity. *Cell*. 2014; 157:1339–1352. [PubMed: 24906151]
- Li P, Fan W, Xu J, Lu M, Yamamoto H, Auwerx J, Sears DD, Talukdar S, Oh D, Chen A, Bandyopadhyay G, Scadeng M, Ofrecio JM, Nalbandian S, Olefsky JM. Adipocyte NCoR knockout decreases PPARgamma phosphorylation and enhances PPARgamma activity and insulin sensitivity. *Cell*. 2011; 147:815–826. [PubMed: 22078880]
- Li XA, Guo L, Dressman JL, Asmis R, Smart EJ. A novel ligand-independent apoptotic pathway induced by scavenger receptor class B, type I and suppressed by endothelial nitric-oxide synthase and high density lipoprotein. *J Biol Chem*. 2005; 280:19087–19096. [PubMed: 15749707]

- Lim YS, McLaughlin T, Sung TC, Santiago A, Lee KF, O'Leary DD. p75(NTR) mediates ephrin-A reverse signaling required for axon repulsion and mapping. *Neuron*. 2008; 59:746–758. [PubMed: 18786358]
- Lyons WE, Mamounas LA, Ricaurte GA, Coppola V, Reid SW, Bora SH, Wihler C, Koliatsos VE, Tessarollo L. Brain-derived neurotrophic factor-deficient mice develop aggressiveness and hyperphagia in conjunction with brain serotonergic abnormalities. *Proc Natl Acad Sci U S A*. 1999; 96:15239–15244. [PubMed: 10611369]
- MacKenzie SJ, Baillie GS, McPhee I, MacKenzie C, Seamons R, McSorley T, Millen J, Beard MB, van Heeke G, Houslay MD. Long PDE4 cAMP specific phosphodiesterases are activated by protein kinase A-mediated phosphorylation of a single serine residue in Upstream Conserved Region 1 (UCR1). *Br J Pharmacol*. 2002; 136:421–433. [PubMed: 12023945]
- Majdan M, Lachance C, Gloster A, Aloyz R, Zeindler C, Bamji S, Bhakar A, Belliveau D, Fawcett J, Miller FD, Barker PA. Transgenic mice expressing the intracellular domain of the p75 neurotrophin receptor undergo neuronal apoptosis. *J Neurosci*. 1997; 17:6988–6998. [PubMed: 9278534]
- Marcinkiewicz A, Gauthier D, Garcia A, Brasaemle DL. The phosphorylation of serine 492 of perilipin A directs lipid droplet fragmentation and dispersion. *J Biol Chem*. 2006; 281:11901–11909. [PubMed: 16488886]
- McConnachie G, Langeberg LK, Scott JD. AKAP signaling complexes: getting to the heart of the matter. *Trends Mol Med*. 2006; 12:317–323. [PubMed: 16809066]
- Minamino T, Orimo M, Shimizu I, Kunieda T, Yokoyama M, Ito T, Nojima A, Nabetani A, Oike Y, Matsubara H, Ishikawa F, Komuro I. A crucial role for adipose tissue p53 in the regulation of insulin resistance. *Nat Med*. 2009; 15:1082–1087. [PubMed: 19718037]
- Monroe JG. Ligand-independent tonic signaling in B-cell receptor function. *Curr Opin Immunol*. 2004; 16:288–295. [PubMed: 15134777]
- O'Rahilly S, Farooqi IS. Genetics of obesity. *Philos Trans R Soc Lond B Biol Sci*. 2006; 361:1095–1105. [PubMed: 16815794]
- Osterreicher CH, Brenner DA. The genetics of nonalcoholic fatty liver disease. *Ann Hepatol*. 2007; 6:83–88. [PubMed: 17519829]
- Osuga J, Ishibashi S, Oka T, Yagyu H, Tozawa R, Fujimoto A, Shionoiri F, Yahagi N, Kraemer FB, Tsutsumi O, Yamada N. Targeted disruption of hormone-sensitive lipase results in male sterility and adipocyte hypertrophy, but not in obesity. *Proc Natl Acad Sci U S A*. 2000; 97:787–792. [PubMed: 10639158]
- Paschos GK, Ibrahim S, Song WL, Kunieda T, Grant G, Reyes TM, Bradfield CA, Vaughan CH, Eiden M, Masoodi M, Griffin JL, Wang F, Lawson JA, Fitzgerald GA. Obesity in mice with adipocyte-specific deletion of clock component Arntl. *Nat Med*. 2012; 18:1768–1777. [PubMed: 23142819]
- Passino MA, Adams RA, Sikorski SL, Akassoglou K. Regulation of hepatic stellate cell differentiation by the neurotrophin receptor p75NTR. *Science*. 2007; 315:1853–1856. [PubMed: 17395831]
- Peeraully MR, Jenkins JR, Trayhurn P. NGF gene expression and secretion in white adipose tissue: regulation in 3T3-L1 adipocytes by hormones and inflammatory cytokines. *Am J Physiol Endocrinol Metab*. 2004; 287:E331–339. [PubMed: 15100092]
- Power RF, Mani SK, Codina J, Conneely OM, O'Malley BW. Dopaminergic and ligand-independent activation of steroid hormone receptors. *Science*. 1991; 254:1636–1639. [PubMed: 1749936]
- Qi L, Saberi M, Zmuda E, Wang Y, Altarejos J, Zhang X, Dentin R, Hedrick S, Bandyopadhyay G, Hai T, Olefsky J, Montminy M. Adipocyte CREB promotes insulin resistance in obesity. *Cell Metab*. 2009; 9:277–286. [PubMed: 19254572]
- Rabizadeh S, Oh J, Zhong LT, Yang J, Bitler CM, Butcher LL, Bredesen DE. Induction of apoptosis by the low-affinity NGF receptor. *Science*. 1993; 261:345–348. [PubMed: 8332899]
- Rosen ED, Spiegelman BM. What we talk about when we talk about fat. *Cell*. 2014; 156:20–44. [PubMed: 24439368]
- Roux PP, Bhakar AL, Kennedy TE, Barker PA. The p75 neurotrophin receptor activates Akt (protein kinase B) through a phosphatidylinositol 3-kinase-dependent pathway. *J Biol Chem*. 2001; 276:23097–23104. [PubMed: 11312266]

- Sachs BD, Baillie GS, McCall JR, Passino MA, Schachtrup C, Wallace DA, Dunlop AJ, MacKenzie KF, Klussmann E, Lynch MJ, Sikorski SL, Nuriel T, Tsigelny I, Zhang J, Houslay MD, Chao MV, Akassoglou K. p75 neurotrophin receptor regulates tissue fibrosis through inhibition of plasminogen activation via a PDE4/cAMP/PKA pathway. *J Cell Biol.* 2007; 177:1119–1132. [PubMed: 17576803]
- Schachtrup C, Ryu JK, Mammadzada K, Khan AS, Carlton PM, Perez A, Christian F, Le Moan N, Vagena E, Baeza-Raja B, Rafalski V, Chan JP, Nitschke R, Houslay MD, Ellisman MH, Wyss-Coray T, Palop JJ, Akassoglou K. Nuclear pore complex remodeling by p75 cleavage controls TGF-beta signaling and astrocyte functions. *Nat Neurosci.* 2015; 18:1077–1080. [PubMed: 26120963]
- Schreyer SA, Cummings DE, McKnight GS, LeBoeuf RC. Mutation of the RIIbeta subunit of protein kinase A prevents diet-induced insulin resistance and dyslipidemia in mice. *Diabetes.* 2001; 50:2555–2562. [PubMed: 11679434]
- Shimomura I, Bashmakov Y, Horton JD. Increased levels of nuclear SREBP-1c associated with fatty livers in two mouse models of diabetes mellitus. *J Biol Chem.* 1999; 274:30028–30032. [PubMed: 10514488]
- Song Y, Altarejos J, Goodarzi MO, Inoue H, Guo X, Berdeaux R, Kim JH, Goode J, Igata M, Paz JC, Hogan MF, Singh PK, Goebel N, Vera L, Miller N, Cui J, Jones MR, Consortium C, Consortium G, Chen YD, Taylor KD, Hsueh WA, Rotter JI, Montminy M. CRT3 links catecholamine signalling to energy balance. *Nature.* 2010; 468:933–939. [PubMed: 21164481]
- Spiegelman BM, Flier JS. Obesity and the regulation of energy balance. *Cell.* 2001; 104:531–543. [PubMed: 11239410]
- Taylor SS, Ilouz R, Zhang P, Kornev AP. Assembly of allosteric macromolecular switches: lessons from PKA. *Nat Rev Mol Cell Biol.* 2012; 13:646–658. [PubMed: 22992589]
- Teng KK, Hempstead BL. Neurotrophins and their receptors: signaling trios in complex biological systems. *Cell Mol Life Sci.* 2004; 61:35–48. [PubMed: 14704852]
- Tran TT, Yamamoto Y, Gesta S, Kahn CR. Beneficial effects of subcutaneous fat transplantation on metabolism. *Cell Metab.* 2008; 7:410–420. [PubMed: 18460332]
- Vilar M, Charalampopoulos I, Kenchappa RS, Reversi A, Klos-Applequist JM, Karaca E, Simi A, Spuch C, Choi S, Friedman WJ, Ericson J, Schiavo G, Carter BD, Ibanez CF. Ligand-independent signaling by disulfide-crosslinked dimers of the p75 neurotrophin receptor. *J Cell Sci.* 2009; 122:3351–3357. [PubMed: 19706676]
- Vischer HF, Leurs R, Smit MJ. HCMV-encoded G-protein-coupled receptors as constitutively active modulators of cellular signaling networks. *Trends Pharmacol Sci.* 2006; 27:56–63. [PubMed: 16352349]
- Wong ST, Henley JR, Kanning KC, Huang KH, Bothwell M, Poo MM. A p75(NTR) and Nogo receptor complex mediates repulsive signaling by myelin-associated glycoprotein. *Nat Neurosci.* 2002; 5:1302–1308. [PubMed: 12426574]
- Xu A, Wang Y, Keshaw H, Xu LY, Lam KS, Cooper GJ. The fat-derived hormone adiponectin alleviates alcoholic and nonalcoholic fatty liver diseases in mice. *J Clin Invest.* 2003a; 112:91–100. [PubMed: 12840063]
- Xu B, Goulding EH, Zang K, Cepoi D, Cone RD, Jones KR, Tecott LH, Reichardt LF. Brain-derived neurotrophic factor regulates energy balance downstream of melanocortin-4 receptor. *Nat Neurosci.* 2003b; 6:736–742. [PubMed: 12796784]
- Yamashita T, Tucker KL, Barde YA. Neurotrophin binding to the p75 receptor modulates Rho activity and axonal outgrowth. *Neuron.* 1999; 24:585–593. [PubMed: 10595511]
- Young KM, Merson TD, Sotthibundhu A, Coulson EJ, Bartlett PF. p75 neurotrophin receptor expression defines a population of BDNF-responsive neurogenic precursor cells. *J Neurosci.* 2007; 27:5146–5155. [PubMed: 17494700]
- Zampieri N, Chao MV. Mechanisms of neurotrophin receptor signalling. *Biochem Soc Trans.* 2006; 34:607–611. [PubMed: 16856873]
- Zechner R, Zimmermann R, Eichmann TO, Kohlwein SD, Haemmerle G, Lass A, Madeo F. FAT SIGNALS--lipases and lipolysis in lipid metabolism and signaling. *Cell Metab.* 2012; 15:279–291. [PubMed: 22405066]

- Zhang HH, Souza SC, Muliro KV, Kraemer FB, Obin MS, Greenberg AS. Lipase-selective functional domains of perilipin A differentially regulate constitutive and protein kinase A-stimulated lipolysis. *J Biol Chem.* 2003; 278:51535–51542. [PubMed: 14527948]
- Zhang P, Smith-Nguyen EV, Keshwani MM, Deal MS, Kornev AP, Taylor SS. Structure and allostery of the PKA RIIbeta tetrameric holoenzyme. *Science.* 2012; 335:712–716. [PubMed: 22323819]
- Zhong H, Sia GM, Sato TR, Gray NW, Mao T, Khuchua Z, Haganir RL, Svoboda K. Subcellular dynamics of type II PKA in neurons. *Neuron.* 2009; 62:363–374. [PubMed: 19447092]
- Zuccaro E, Bergami M, Vignoli B, Bony G, Pierchala BA, Santi S, Cancedda L, Canossa M. Polarized expression of p75(NTR) specifies axons during development and adult neurogenesis. *Cell Rep.* 2014; 7:138–152. [PubMed: 24685135]

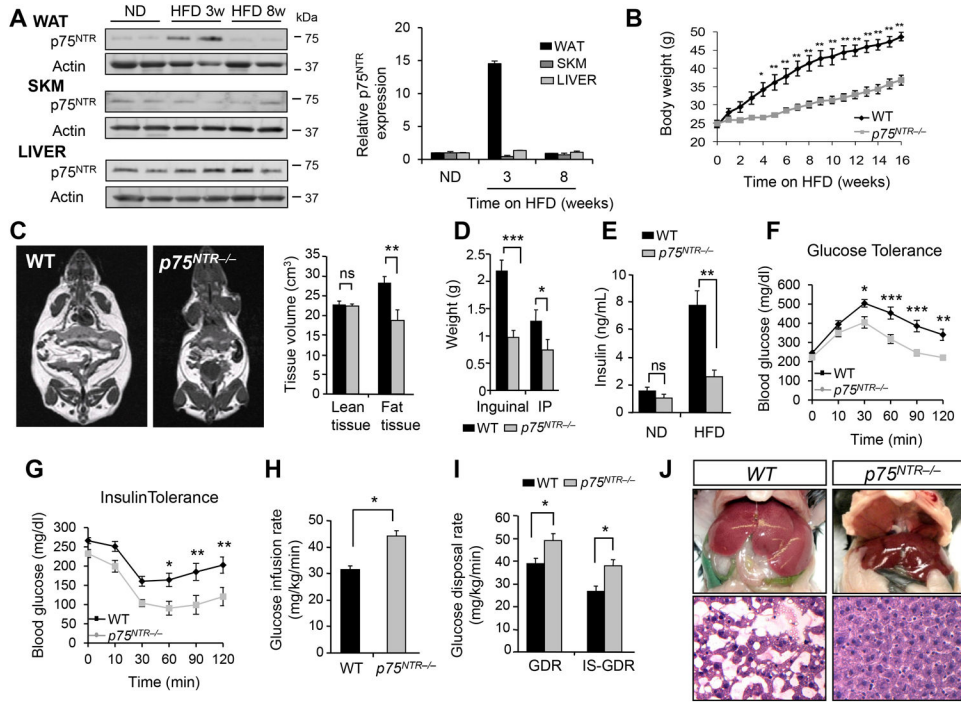


Figure 1. p75^{NTR} Deficiency Protects Mice from HFD-Induced Obesity and Metabolic Syndrome (A) p75^{NTR} protein (left) and RNA (right) expression in WAT, skeletal muscle (SKM), and liver from WT and p75^{NTR}^{-/-} mice on ND (normal diet) and, 3 and 8 weeks on HFD. Representative immunoblot is shown from three independent experiments.

(B) Body weight of WT and p75^{NTR}^{-/-} mice on HFD (**P* < 0.01, ***P* < 0.001, two-way ANOVA; *n* = 7 mice per group).

(C) Representative MRI images of WT and p75^{NTR}^{-/-} mice on HFD (left) and tissue volumes of WT and p75^{NTR}^{-/-} mice on HFD (right) (***P* < 0.01, ns: not significant, unpaired Student's *t*-test; *n* = 7 mice per group).

(D) Weights of WT and p75^{NTR}^{-/-} inguinal and intraperitoneal (IP) fat on HFD (**P* < 0.05, ****P* < 0.001, unpaired Student's *t*-test; *n* = 7 mice per group).

(E) Basal insulin levels from WT and p75^{NTR}^{-/-} mice (***P* < 0.01, ns, unpaired Student's *t*-test; *n* = 4 mice per group).

(F) Glucose and (G) insulin tolerance test in WT (*n* = 13) and p75^{NTR}^{-/-} (*n* = 8) mice after 20 weeks on HFD (**P* < 0.05, ***P* < 0.01, ****P* < 0.001, two-way ANOVA).

(H) Glucose infusion rates from WT (*n* = 5) and p75^{NTR}^{-/-} (*n* = 7) mice on HFD (**P* < 0.05, unpaired Student's *t*-test).

(I) Total and insulin-stimulated glucose disposal rate (GDR) of WT (*n* = 5) and p75^{NTR}^{-/-} (*n* = 7) mice on HFD (**P* < 0.05, unpaired Student's *t*-test).

(J) Representatives photographs (top) and histological images (bottom) of livers from WT and p75^{NTR}^{-/-} mice on HFD (*n* = 3 mice per group).

See also Figures S1 and S2.

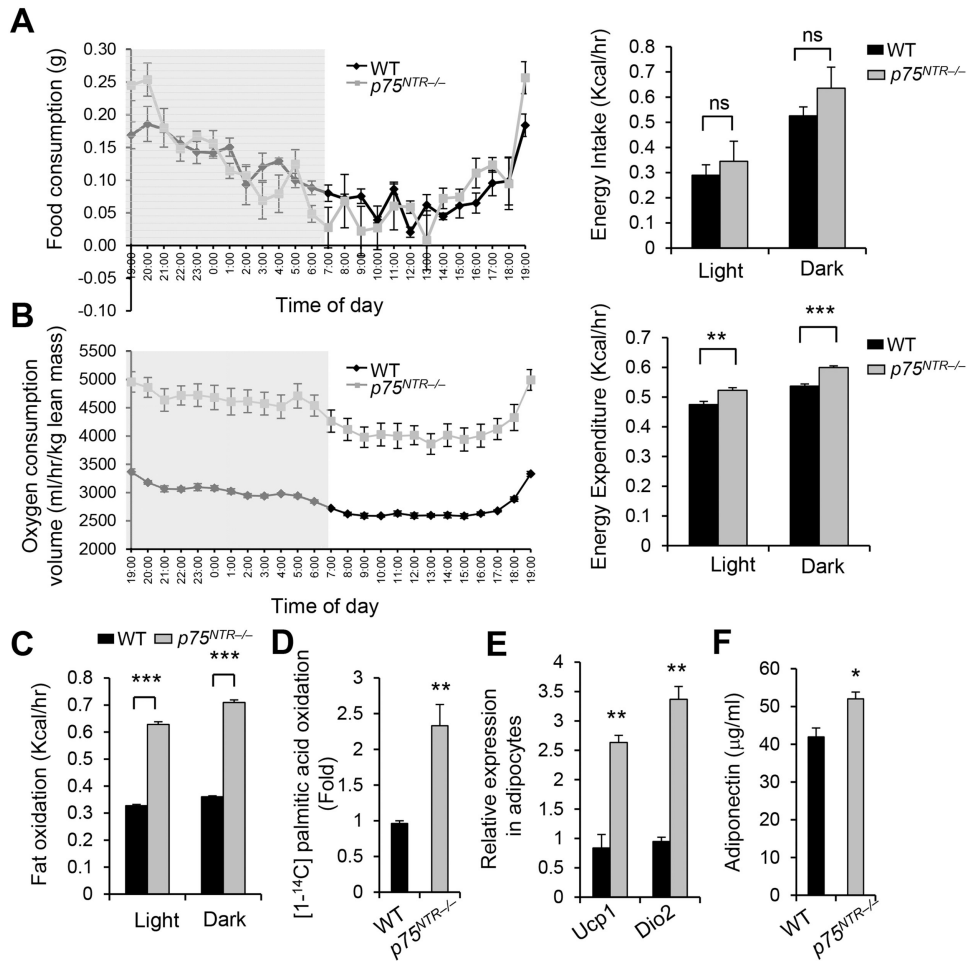


Figure 2. *p75^{NTR}* Deficiency Increases Energy Expenditure, Fat Oxidation, and Lipolysis
 (A) Food consumption (left) and energy intake (right) of WT ($n = 7$) and *p75^{NTR}*^{-/-} ($n = 8$) mice on HFD (ns: not significant, unpaired Student's *t*-test).
 (B) Oxygen consumption (left) and energy expenditure (right) normalized to lean body mass in WT ($n = 7$) and *p75^{NTR}*^{-/-} ($n = 8$) mice on HFD (** $P < 0.01$, *** $P < 0.001$, Student's *t*-test).
 (C) Fat oxidation normalized to lean body mass in WT and *p75^{NTR}*^{-/-} mice on HFD (*** $P < 0.001$, unpaired Student's *t*-test; $n = 6$ mice per group).
 (D) Oxidation of [1-¹⁴C]-palmitate to ¹⁴CO₂ by adipocytes isolated from WT and *p75^{NTR}*^{-/-} mice (** $P < 0.01$, unpaired Student's *t*-test). Results are from three independent experiments.
 (E) Ucp1 and Dio2 RNA expression in primary adipocytes from WT and *p75^{NTR}*^{-/-} mice (** $P < 0.01$, unpaired Student's *t*-test; $n = 6$ mice per group).
 (F) Serum levels of adiponectin in WT and *p75^{NTR}*^{-/-} mice on HFD (* $P < 0.05$, unpaired Student's *t*-test; $n = 3$ mice per group).
 See also Figures S3 and S4.

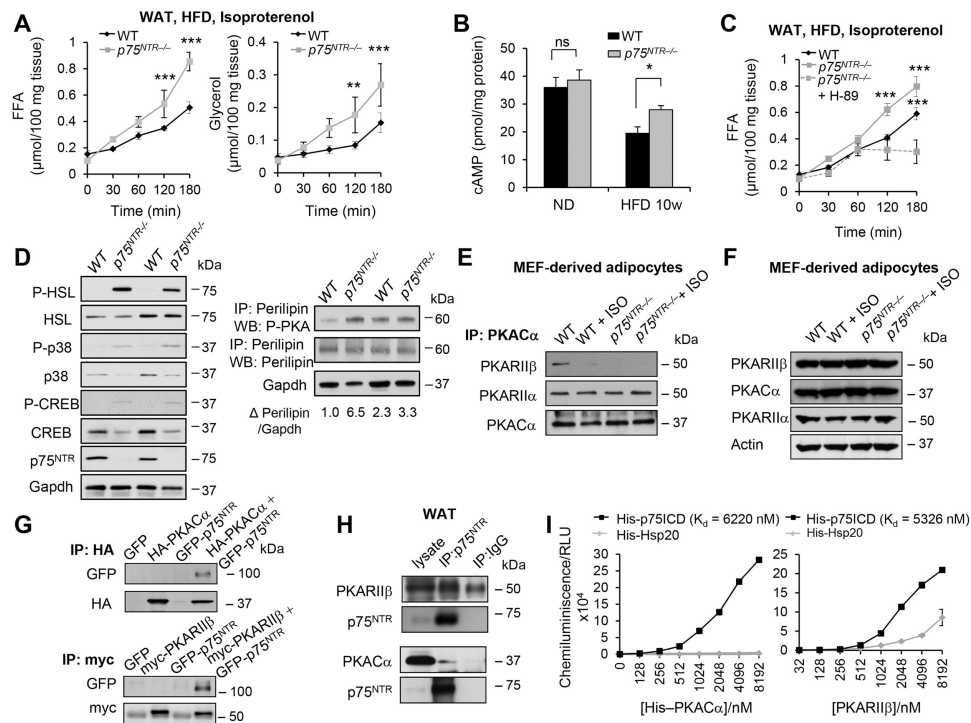


Figure 3. $p75^{NTR}$ Regulates Lipolysis via cAMP/PKA Signaling

(A) Isoproterenol-stimulated FFA and glycerol levels in WAT from WT and $p75^{NTR-/-}$ mice on HFD (** $P < 0.01$, *** $P < 0.001$, two-way ANOVA; $n = 8$ mice per group).

(B) cAMP accumulation in WAT from WT and $p75^{NTR-/-}$ mice on normal chow (ND) or 10 weeks on HFD (* $P < 0.05$, ns: not significant, unpaired Student's t -test; $n = 4$ mice per group).

(C) FFA levels in WAT treated with the PKA inhibitor, H-89 from WT, and $p75^{NTR-/-}$ mice on HFD (WT or $p75^{NTR-/-}$ vs $p75^{NTR-/-}$ treated with H-89, *** $P < 0.001$, two-way ANOVA; $n = 5$ mice per group).

(D) P-HSL, HSL, P-p38, p38, P-CREB, CREB, and $p75^{NTR}$ protein expression (left) and immunoprecipitation of lysates with anti-perilipin followed by Western blotting with anti-phospho-PKA (p-PKA) to detect all PKA-phosphorylation sites on perilipin and total perilipin expression ($n = 2$ mice per group) (right) in WAT from WT and $p75^{NTR-/-}$ mice on HFD. Phospho-perilipin levels normalized to GAPDH were quantified by densitometry (represents fold changes). Representative immunoblots are shown from $n = 12$ mice per group.

(E) Immunoprecipitation of PKA-C α protein followed by Western blotting to detect PKA RII β and RII α from WT and $p75^{NTR-/-}$ MEF-derived adipocytes treated or not with isoproterenol (ISO). Representative immunoblot from three independent experiments.

(F) PKA-C α , PKA-RII β , and PKA-RII α protein expression in WT and $p75^{NTR-/-}$ MEF-derived adipocytes. Representative immunoblots from three independent experiments.

(G) Immunoprecipitation of HA-PKA-C α protein (top) and myc-PKA-RII β (bottom) followed by Western blotting to detect GFP- $p75^{NTR}$ in 293T cells overexpressing indicated constructs. Representative immunoblots from three independent experiments.

(H) Immunoprecipitation of PKA-RII β (top) and PKA-C α (bottom) protein followed by Western blotting to detect p75^{NTR} in WAT from WT mice. Representative immunoblots from three independent experiments.

(I) ELISA binding assays between recombinant His-p75ICD and increasing concentrations of His-PKA-C α (left) and PKA-RII β (right). His-Hsp20 was used as a control. Results are from 3 independent experiments performed with duplicates. K_d values were estimated using a one-site binding model.

See also Figure S5.

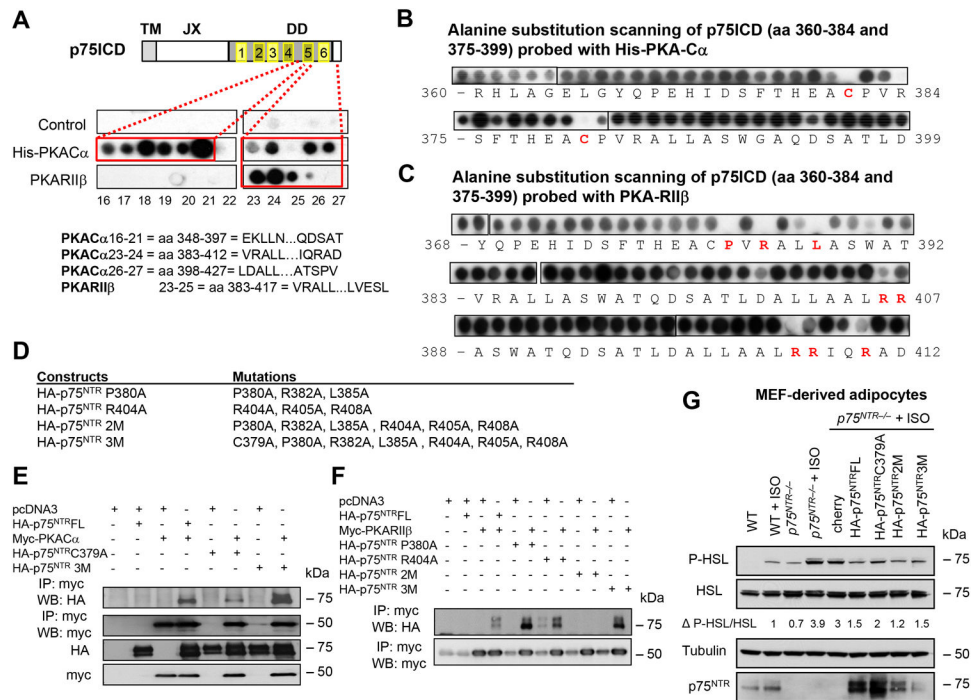


Figure 4. p75^{NTR} Interacts with the PKA Catalytic (C α) Subunit to Regulate Lipolysis

(A) Peptide array mapping of the p75ICD sites required for the interaction with PKA-C α and PKA-RII β . Schematic diagram of p75ICD shows the domain organization and peptide location, length, and sequences.

(B) Alanine scanning substitution arrays of the identified interacting p75^{NTR} peptides 360–384 and 375–399 probed with PKA-C α . Red amino acids indicate substitutions that block the interaction.

(C) Alanine scanning substitution arrays of interacting p75^{NTR} peptides 368–392, 383–407, and 388–412 probed with PKA-RII β . Highlighted in red are the amino acids whose substitution blocks the interaction.

(D) p75^{NTR} mutant constructs generated.

(E) Immunoprecipitation of myc-PKA-C α protein followed by Western blotting to detect HA-p75^{NTR} wild-type and HA-p75^{NTR}C379A or HA-p75^{NTR} 3M in 293T cells overexpressing indicated constructs. Representative immunoblots are shown from three independent experiments.

(F) Immunoprecipitation of myc-PKA-RII β protein followed by Western blotting to detect HA-p75^{NTR} wild-type and HA-p75^{NTR} P380A, HA-p75^{NTR} R404A, HA-p75^{NTR} 2M, or HA-p75^{NTR} 3M in 293T cells overexpressing indicated constructs. Representative immunoblots from three independent experiments.

(G) P-HSL, HSL, and p75^{NTR} protein expression in WT and p75^{NTR}-/- MEF-derived adipocytes infected with lentiviral vectors overexpressing the indicated constructs and treated or not with isoproterenol (ISO). Representative immunoblots from three independent experiments.

See also Figure S6.

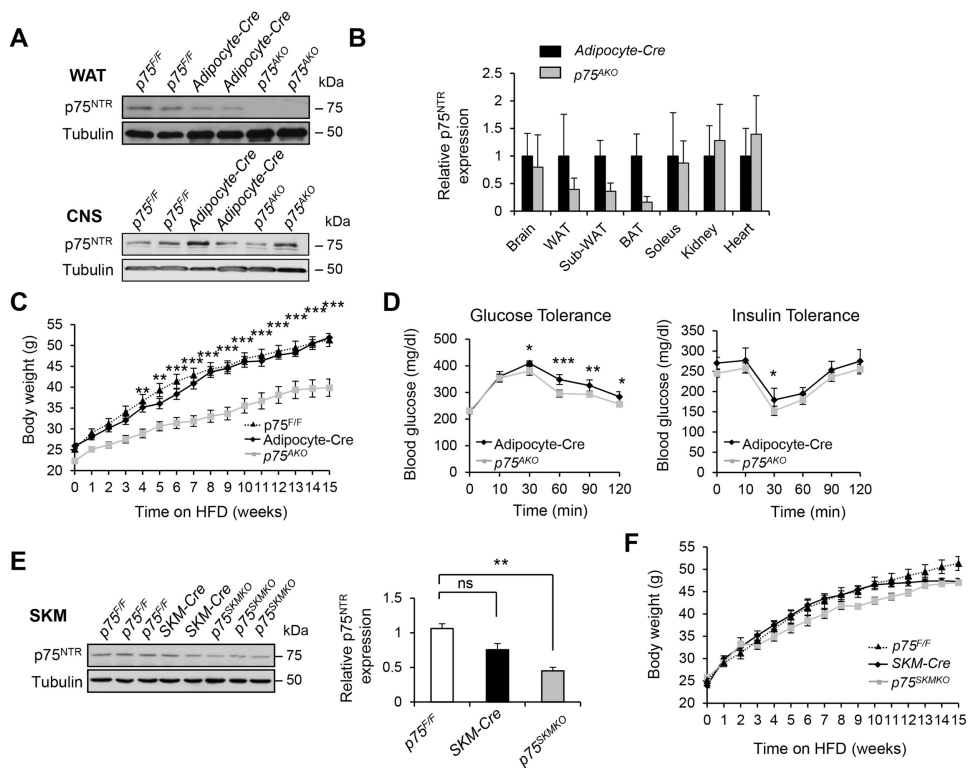


Figure 5. p75^{NTR} Deficiency in WAT Protects Mice from HFD-induced Obesity and Insulin Resistance

(A) p75^{NTR} protein expression in WAT and the central nervous system (CNS) from p75^{F/F}, Adipocyte-cre, and p75^{AKO} mice. Representative blot is shown from two independent experiments ($n = 5$ mice per group).

(B) p75^{NTR} expression in brain, WAT (epididymal fat), SUBC (subcutaneous inguinal fat), BAT (brown adipose tissue), Soleus (skeletal muscle), kidney, and heart from Adipocyte-cre and p75^{AKO} mice ($n = 5$ mice per group).

(C) Body weight of p75^{F/F} ($n = 18$), Adipocyte-cre ($n = 7$), and p75^{AKO} ($n = 10$) mice on HFD (** $P < 0.01$, *** $P < 0.001$, two-way ANOVA).

(D) Glucose (left) and insulin tolerance (right) tests in Adipocyte-cre ($n = 7$) and p75^{AKO} ($n = 10$) mice after 8 weeks on HFD (* $P < 0.05$, ** $P < 0.01$, *** $P < 0.001$, two-way ANOVA).

(E) p75^{NTR} protein expression in skeletal muscle from p75^{F/F} ($n = 3$), SKM-cre ($n = 2$), and p75^{SKM/KO} mice (left) ($n = 3$). Quantifications of Western blot analysis for p75^{NTR} in skeletal muscle from p75^{F/F}, MCK-cre, and p75^{SKM/KO} mice (ns, not significant; * $P < 0.05$, Tukey's multiple comparisons test one-way ANOVA analysis) (right).

(F) Body weight of p75^{F/F} ($n = 18$), SKM-cre ($n = 10$), and p75^{SKM/KO} ($n = 15$) mice on HFD (not significant, two-way ANOVA).

See also Figure S7.

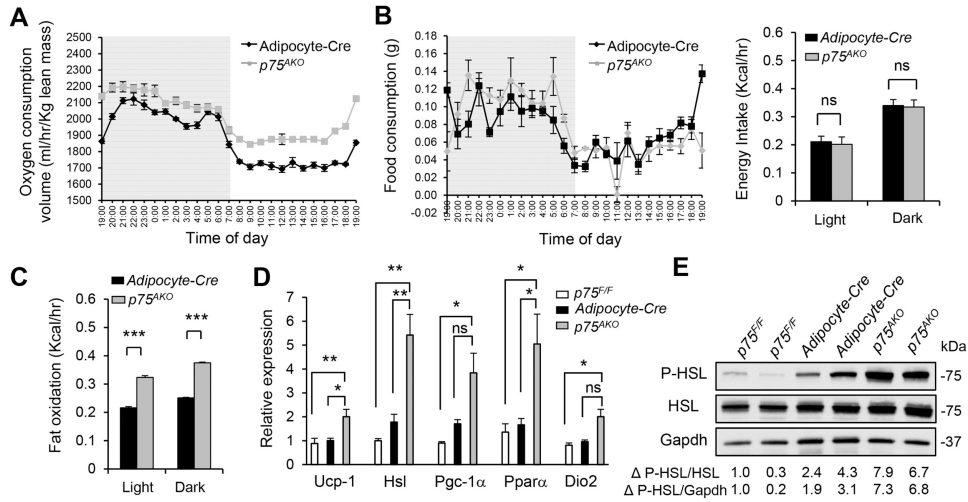


Figure 6. p75^{NTR} Deficiency in WAT Increases Thermogenesis and Lipolysis
 (A) Oxygen consumption normalized to lean body mass in *Adipocyte-cre* and *p75^{AKO}* mice on HFD ($n = 6$ mice per group).
 (B) Food consumption (left) and energy intake (right) of *Adipocyte-cre* ($n = 10$) and *p75^{AKO}* ($n = 12$) mice over 4 days after 10 weeks of HFD (ns: not significant, unpaired Student's t -test).
 (C) Fat oxidation normalized to lean body mass in *Adipocyte-cre* and *p75^{AKO}* mice on HFD ($***P < 0.001$, unpaired Student's t test; $n = 6$ mice per group).
 (D) *Ucp1*, *Hsl*, *Pgc-1α*, *Pparaα*, and *Dio2* RNA expression in WAT from *p75^{F/F}*, *Adipocyte-cre*, and *p75^{AKO}* mice on HFD (ns: not significant, $*P < 0.05$, $**P < 0.01$, Tukey's multiple comparisons test one-way ANOVA analysis; $n = 4$ mice per group).
 (E) P-HSL and HSL protein expression in WAT from *p75^{F/F}* ($n = 2$), *Adipocyte-cre* ($n = 3$), and *p75^{AKO}* ($n = 2$) mice on HFD.
 See also Figure S7.

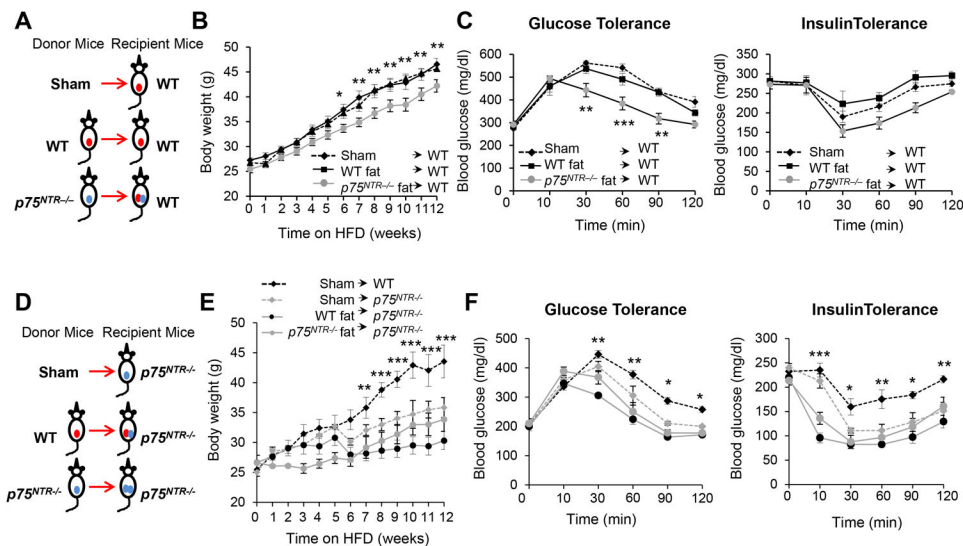


Figure 7. $p75^{NTR}$ -deficient WAT Transplantation Reduces Body Weight and Insulin Resistance
 (A) Schematic of fat transplantation for WT mice. Epididymal fat from $p75^{NTR-/-}$, WT, and no fat (sham) was transplanted in WT mice. All animals after surgery were fed a HFD.
 (B) Body weight of WT mice transplanted with $p75^{NTR-/-}$ fat ($n = 9$), WT fat ($n = 9$) and sham ($n = 5$). (WT→WT vs $p75^{NTR-/-}$ →WT, * $P < 0.05$, ** $P < 0.01$ by two-way ANOVA).
 (C) Glucose (left) and insulin tolerance (right) tests in WT-transplanted mice after 8 weeks on HFD. ($p75^{NTR-/-}$ →WT vs WT→WT, ** $P < 0.01$, *** $P < 0.001$ by two-way ANOVA; $n = 4$).
 (D) Schematic of fat transplantation. Epididymal fat from $p75^{NTR-/-}$, WT, and no fat (sham) was transplanted in $p75^{NTR-/-}$ mice. All animals after surgery were fed a HFD.
 (E) Body weight of WT and $p75^{NTR-/-}$ mice transplanted with $p75^{NTR-/-}$ ($n = 9$) or WT fat ($n = 9$) and sham-operated ($n = 4$). (WT sham vs WT→ $p75^{NTR-/-}$ ** $P < 0.01$, *** $P < 0.001$, two-way ANOVA).
 (F) Glucose (left) and insulin tolerance (right) tests in recipient mice after 10 weeks of HFD (WT sham vs WT→ $p75^{NTR-/-}$, * $p < 0.05$, ** $P < 0.01$, *** $P < 0.001$, two-way ANOVA; $n = 4$ mice per group).